Journal of Laser Applications

RESEARCH ARTICLE | FEBRUARY 15 2023

Powder catchment efficiency in laser cladding (directed energy deposition). An investigation into standard laser cladding and the ABA cladding technique

Daniel Koti ✉; John Powell; Himani Naesstroem; ... et. al

Check for updates

Journal of Laser Applications 35, 012025 (2023)
https://doi.org/10.2351/7.0000904

CrossMark

View Online

Export Citation

Articles You May Be Interested In

Influence of writing and reading intertrack interferences in terms of bit aspect ratio in shingled magnetic recording

Journal of Applied Physics (February 2014)

Simulation of runoff using HEC-HMS for ungauged catchment

AIP Conference Proceedings (July 2021)

Powder catchment in laser metal deposition

Journal of Laser Applications (April 2019)

ALIA THE LASER INSTITUTE Journal of Laser Applications

Learn More

RAPID TIME TO ACCEPTANCE

COMMUNITY DRIVEN

EXPANSIVE COVERAGE

PRESTIGIOUS EDITORIAL BOARD

EXTENSIVE MARKETING

ALIA THE LASER INSTITUTE

Downloaded from http://pubs.aip.org/lia/jla/article-pdf/doi/10.2351/7.0000904/16705003/012025_1_online.pdf

Journal of Laser Applications ARTICLE scitation.org/journal/jla

Powder catchment efficiency in laser cladding (directed energy deposition). An investigation into standard laser cladding and the ABA cladding technique

Cite as: J. Laser Appl. **35**, 012025 (2023); doi: 10.2351/7.0000904
Submitted: 6 November 2022 · Accepted: 27 January 2023 ·
Published Online: 15 February 2023

View Online Export Citation CrossMark

Daniel Koti,[1,a)] John Powell,[1,2] Himani Naesstroem,[3] and K. T. Voisey[1]

AFFILIATIONS

[1]Faculty of Engineering, University of Nottingham, University Park, Nottingham NG7 2RD, United Kingdom
[2]Innovation Campus Future Mobility, University of Stuttgart, ICM, D-70569 Stuttgart, Germany
[3]Department of Engineering Sciences and Mathematics, Lulea University of Technology, 97187 Lulea, Sweden.

Note: This paper is part of the Special Collection: Laser Additive Manufacturing Processes: From Cladding to Complex Parts.
[a)]Author to whom correspondence should be addressed; electronic mail: daniel.koti@nottingham.ac.uk.
Telephone: +44-751-238-4934

ABSTRACT

This paper investigates the efficiency of powder catchment in blown powder laser cladding (a directed energy deposition technique). A comparison is made between standard "track by overlapping track" cladding ("AAA" cladding) and "ABA" cladding, where the gaps left between an initial set of widely spaced tracks ("A" tracks), are filled in by subsequent "B" tracks. In both these techniques, the melt pool surface is the collection area for the cladding powder, and the shape of this pool can be affected by several parameters including cladding speed, intertrack spacing, and type of cladding technique. The results presented here are derived from of an analysis of high-speed videos taken during processing and cross sections of the resultant clad tracks. The results show that the first track in AAA cladding has a different melt pool shape to subsequent tracks, and that the asymmetry of the subsequent track melt pools results in a reduction in the powder catchment efficiency. In contrast to this, the geometry of the "B" track melt pools between their adjacent "A" tracks results in an enhanced powder catchment efficiency.

Key words: directed energy deposition, laser cladding, ABA laser cladding, fibre laser, melt pool shape. high speed imaging. powder catchment efficiency

© 2023 Author(s). All article content, except where otherwise noted, is licensed under a Creative Commons Attribution (CC BY) license (http://creativecommons.org/licenses/by/4.0/). https://doi.org/10.2351/7.0000904

Downloaded from http://pubs.aip.org/lia/jla/article-pdf/doi/10.2351/7.0000904/16705003/012025_1_online.pdf

I. INTRODUCTION

Investigations into laser cladding [a directed energy deposition (DED technique] began in the late 1970s and early 1980s,[1–3] and the process has grown to achieve industrial status, particularly with the development of additive manufacturing. Nowadays, the process commonly utilizes a processing head that supplies a stream of the cladding powder alloy coaxially with a defocused laser beam.[4] One of the aims of the process is to melt all of the powder which arrives at the laser-material interaction area into the clad track. Unfortunately, complete capture of all the incoming powder is not generally possible, and a certain percentage of powder escapes the process, often by deflection off the solid material beyond the edges of the melt pool or the surface of the melt pool itself.[5]

The powder catchment efficiency of the process has a strong influence on costs and is thus of prime importance to industrial users. This efficiency is simply the percentage of powder provided to the process which becomes part of the laser melted clad layer.

© Author(s) 2023

For technical investigations, the powder catchment efficiency (E_{pc}) of any individual clad track can be calculated using cross sections of the clad layer and knowledge of the process parameters as follows:

$$E_{pc}(\%) = ((T_{area} \times v \times \rho)/F_p) \times 100, \quad (1)$$

where E_{pc} is the powder catchment efficiency (%), T_{area} is the cross-sectional area of the track above the original line of the substrate surface (mm^2), v is the process speed (mm/min), ρ is the density of cladding material (g/mm^3), F_p is the powder feed rate (g/min).

Table I presents a small, but typical, sample of the results of a survey of investigations into DED laser cladding over a wide range of process parameters and different laser types, which reveals that E_{pc} can often be well below 50%. This is clearly a problem as the powder is expensive and unused powder cannot generally be recycled into the cladding process, which depends upon high levels of powder uniformity.

Standard laser cladding involves laying down an initial track on the substrate surface [an "A" track—see Fig. 1(a)] and many research investigations simply compare single tracks of this type laid down under different processing conditions (in this paper, we will refer to this type of deposit as a "solo "A" track"). In industrial practice however, single tracks of this type have very limited application as it is much more common to overlap track one with track two, then track three, etc., until the required clad surface is achieved, as shown in Fig. 1(b) (for obvious reasons, we can refer to this technique as "AAA cladding"). Recent work by the authors of Ref. 29 has shown that there are E_{pc} benefits to be gained if a new laser cladding technique, which we have called "ABA laser cladding," is employed.

In ABA cladding the coverage strategy is to lay down a sequence of widely separated, identical tracks (the "A" tracks), and then fill the gaps between them with "B" tracks [see Fig. 1(c)].

Early work on ABA cladding[29] has revealed that several benefits can arise from utilizing the technique, including; improved powder catchment efficiency (E_{pc}), the avoidance of a "start-up zone" for the process [see Fig. 1(b)] and the fact that different alloys could be used for the "A" and "B" tracks. The improvement in E_{pc} (see Fig. 2) results in less powder wastage and increased coverage rates for the process, and, therefore, reduced costs.

E_{pc} of the laser cladding process is fundamentally governed by how much powder enters the cladding melt pool, which is, in turn, influenced by the size and shape of the melt pool surface. The size and shape of the melt pool surface can be affected by laser power, cladding speed, powder feed rate, etc. In this work, we investigate, for a single clad layer, the influence of cladding technique (AAA or ABA), intertrack spacing, and cladding speed on melt pool surface geometry and the effect of that geometry on E_{pc}.

TABLE I. Powder catchment efficiencies calculated from published results in the literature.

Papers	Substrate	Powder	Laser power (kW)	Powder feed rate (g/min)	Process speed (m/min)	Beam diameter (mm)	Powder catch. Eff (%)
6	Zr alloy	Zr	0.8	8.8	0.245	1.4	9.09
7	AISI 1050	AISI 316L	0.8–1	8.16–16.26	0.288–0.48	2.2	12–16
8	AISI 316L	AISI 316L	0.525–0.7	6–13	1.32–2.52	1.2	20–32
9	Inconel 625	Inconel 625	1–1.5	4.55–7.6	0.3–0.8	2	28–40
10	Inconel 718	Inconel 718	0.35–0.55	1.2	0.6	1	28–45
11	S235JRC + C	1.4313	1.2	14–16	0.8–1	2	34–42
12	AISI 316L	Inconel 625	3.2	50.91	24.96	5	42.16
13	A45	Ni60	3.2	50.91	24.96	2	43.14
14	SS304	Eutroloy 16012	1	9	0.3	3	49.88
15	Q235	Fe-based alloy	1.1	8.5	0.3	4	55.8
16	A36	Fe-based	3–4.5	40–60	0.18–0.42	3.38	51–68
17	Inconel 625	Inconel 625	2.5	19	0.636	4	60.77
18	S235JR	Inconel 625	15	295	0.75	5	77
19	Ti811	Ni60	0.9	5	0.5	3	78.61
20	CuBe alloy	AISI H13	3.6	3.2	18.2	3	79.63
21	S235JR	Inconel 625	15	273	1	5	79.98
22	AISI 304	AISI 316L	1.5–2	8.5–17	0.3–0.6	3	80
23	AISI 420	Stellite 6	0.72	22	3	2	80.11
24	SNCrW	EuTroLoy 16006	4	20	0.24	2	80.34
25	AISI 1045	Inconel 625	3.131	40	1.545	2	82.2
26	SNCrW	EuTroLoy 16006	4	20	0.24	2	86.25
27	Mild steel	Hastelloy C	2.4	28	1.4	4	86.78
28	Inconel 718	Inconel 718	2.9	45	1.5	4	92.04

Downloaded from http://pubs.aip.org/lia/jla/article-pdf/doi/10.2351/7.0000904/16705003/012025_1_online.pdf

© Author(s) 2023

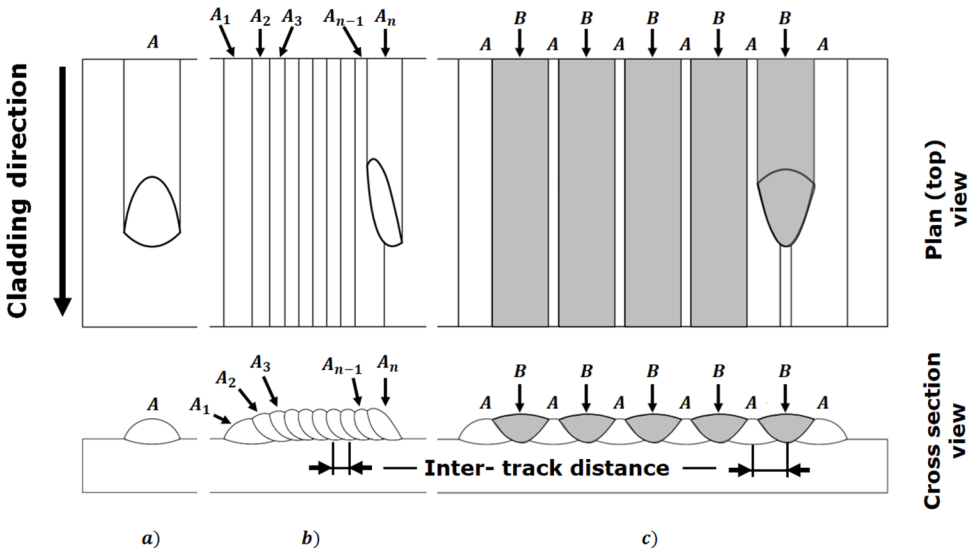

FIG. 1. (a) A solo, or initial, "A" track, (b) In standard (AAA) laser cladding the clad surface is made up of overlapping "identical" tracks (although a few, early tracks differ from later tracks), (c) in ABA cladding, a set of widely spaced identical "A" tracks are laid down first and then the gaps between them are filled with "B" tracks.

II. EXPERIMENTAL DETAILS

A. Cladding parameters

Laser cladding measurements were conducted with a 15 kW IPG Ytterbium-doped, cw fiber laser [1070 nm wavelength, 150 mm collimating lens and Kugler mirror optics (Kugler LK390F) with a 250 mm focussing mirror]. The laser system used a fiber with a diameter of 100 μm, coupled to a fiber with a diameter of 400 μm. The laser power used during the experiments was 3 kW. The beam was defocused into a circular spot measuring approximately 4 mm in diameter with a Gaussian energy distribution and a stand-off distance of 13 mm.

A coaxial COAX 14V5 (Fraunhofer IWS) 8 mm diameter continuous nozzle (also known as a ring-slit nozzle) was employed. The carrier gas and the powder were fed through the ring-shaped slit, and the laser beam and shielding gas passed through the central nozzle. This produced a focussed powder feeding stream with a diameter of approximately 2 mm at the melt pool surface.

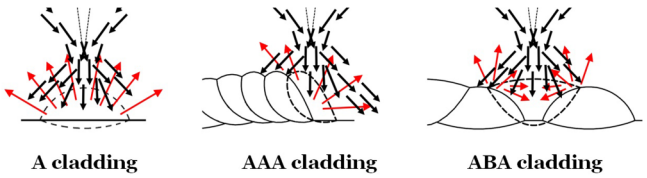

FIG. 2. In AAA cladding, a considerable percentage of the powder can be deflected away from the melt pool. ABA cladding geometry is more favorable to powder capture.

Argon was used for shielding and as the carrier gas. 316L stainless steel powder with a size range from 50 to 150 μm diameter was fed from a gravity-based powder feeder. The carrier gas flow was 8 l/min and shielding gas flow was 15 l/min. The powder feeder was calibrated, and the feed rate was set at 26 g/min throughout the experiment. This feed rate was checked experimentally twice by collecting the powder in a specially designed container over a 5-minute period, with a standard deviation on 26 g/min of 0.08. The laser cladding was carried out on a three-axis ISEL FlatCOM L150 CNC system with the substrate plates (5 mm thick 304S15 stainless steel) clamped to a linear motion table. Both the laser head and the powder feeder nozzle were attached to the z axis and remained fixed.

Tracks were created using both the AAA and ABA techniques with a range of intertrack (center to center, see Fig. 1) spacings of between 2 and 4 mm. The tracks comparing "AAA" and "ABA" clads were carried out at 700 mm/min.

For further investigation into ABA cladding, the process speed was varied between 700 and 1500 mm/min. A series of solo "A" tracks were also made over this range to investigate pool shape changes as a function of process speed. The clad samples were sectioned, polished, and etched in aqua regia.

B. High-speed imaging

The process was recorded using a high-speed imaging (HSI) camera at 8000 frames per second. Illumination was provided by a continuous wave diode illumination laser with a wavelength of 808 nm. A narrow bandwidth filter matching the wavelength of the illumination laser was used to block out the process light. The process setup is illustrated in Fig. 3. The camera was inclined at 11°

Downloaded from http://pubs.aip.org/lia/jla/article-pdf/doi/10.2351/7.0000904/16705003/012025_1_online.pdf

© Author(s) 2023

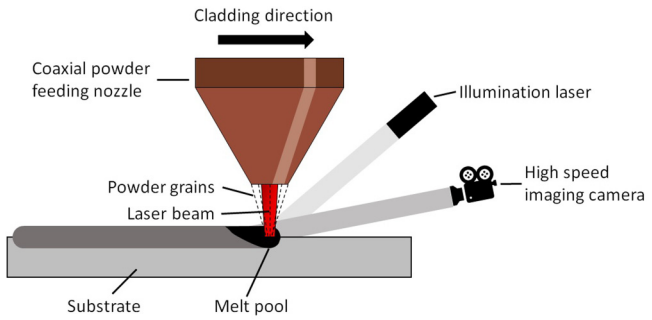

FIG. 3. High speed imaging experimental setup.

from the horizontal. High-speed imaging videos were played back at low frame rates to observe powder catchment behavior and melt pool geometry.

Figure 4 shows how the plan view maps of the melt pools were extracted from the video data (in this example, for a solo "A" track). The maximum width of the melt pool can be measured directly from the video, but its length iL needs to be calculated using Eq. (2) (refer to Fig. 4),

$$L = (D - (H \times \cos(\theta)))/\sin(\theta). \quad (2)$$

Once L and the maximum width are known, then the overall shape of the pool perimeter can be taken from the video data and the plan (top) view of the melt pool mapped. The plan view was preferred to the view perpendicular to the melt surface because the powder can be assumed to be falling vertically downwards.

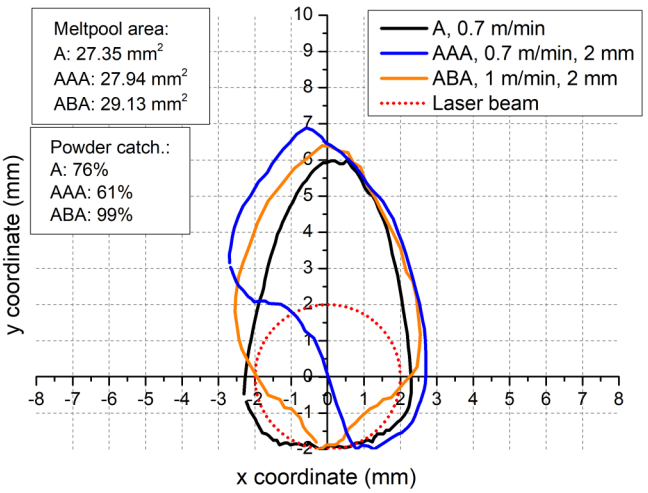

FIG. 5. Melt pool shapes (plan, or top view, i.e., mapped in the plane parallel to the substrate surface) for different laser cladding interaction types. In these maps, the part of the melt pool at the bottom of the figure is the front, or leading edge, of the melt pool (i.e., the melt pool is portrayed as moving downwards along the y axis in this figure). The laser beam (shown as a dotted circle) is centered on the x,y 0,0 point. The information on the top right gives details of the process speed and inter-track separation distance (see Fig. 1).

III. RESULTS AND DISCUSSION

A. Differences in melt pool shape between A, AAA, and ABA cladding techniques

Figure 5 provides interesting information about the differences in melt pool shape as a function of cladding technique. The information labeled "A" refers to; solo "A" tracks, any of the "A" tracks in ABA cladding, and also to the initial track in AAA cladding.

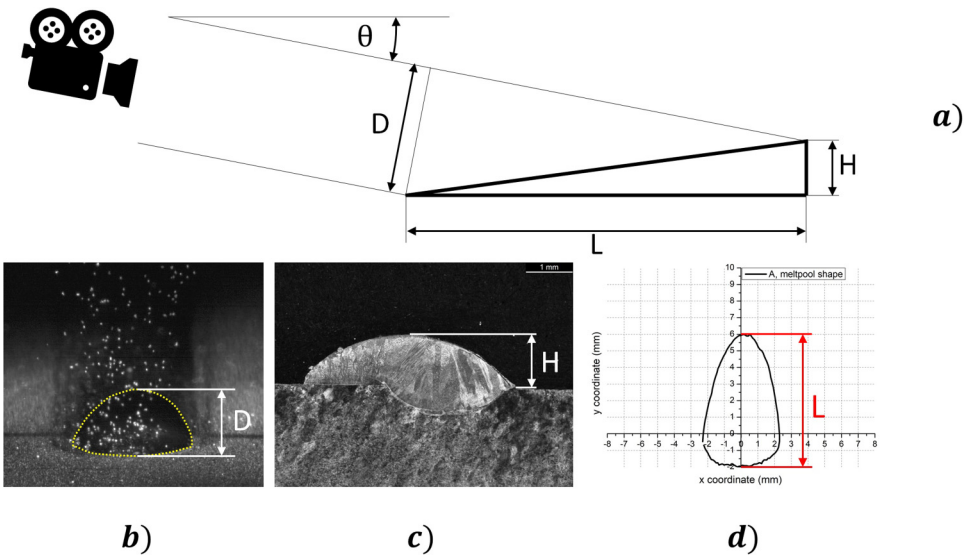

FIG. 4. (a) A schematic of the video capture geometry. (b) A typical single frame from the video ("A" track). (c) A typical "A" track cross section. (d) A typical calculated melt pool geometry (plan view "A" track).

Downloaded from http://pubs.aip.org/lia/jla/article-pdf/doi/10.2351/7.0000904/16705003/012025_1_online.pdf

© Author(s) 2023

These "A" tracks are laid down upon the flat substrate surface and therefore have the simplest melt pool geometry (see Fig. 1). The information labeled "AAA" refers to any one of the tracks which follow the initial track in AAA cladding. In this experiment, we measured and made a high-speed video of track A_3 (see Fig. 1). The information labeled "ABA" refers only to the "B" tracks in ABA cladding.

The cladding process speeds and intertrack distances (see Fig. 1) for the tracks compared here are given in the figure.

The melt pool associated with single clad tracks produced on a flat surface (the "A" tracks) is, as we would expect, symmetric about the central axis in the direction of cladding. It is also broadest near the front, in the vicinity of the laser beam, and tapers off behind the laser beam as the melt pool solidifies from the outside edges toward the middle. This melt pool shape is the one created in all the A tracks laid down in ABA cladding and the initial track in AAA cladding.

The melt pool associated with the tracks which follow this initial track in AAA cladding (labeled "AAA" in Fig. 5) has a completely different shape to the initial A track pool. At the leading edge, on the side of the pool which is on the flat substrate surface (the bottom right-hand side in the figure), the melt pool shape is similar to (but slightly wider than) the single A track pool. On the left-hand side of the leading edge however, the melt front is initiated a few millimeters later in the laser–material interaction. This is because, on this side, the melt is being generated on the "shoulder" of the previous track. The geometry of this shoulder means that the intensity of the incident beam is reduced in this area, because it is incident on a sloping, curved surface [see Fig. 6(b)] and, because of this, the melting takes more time to initiate.

Figure 6 demonstrates how the relative beam intensity varies as a function of the slope of the previous track, but the situation has been simplified to assume a square cross section laser beam with a top hat mode. In reality, the beam has a Gaussian energy distribution and a circular cross section. Both of these points mean that the reduction of energy absorbed by the sloping surface will be accentuated. A full model of the situation would also have to take into account the temperature of the substrate (as absorptivity can be temperature dependent). To add to the complication of such a model, the absorption coefficient of the laser beam is also dependent on the angle of incidence, although this will tend to reduce rather than accentuate the trend shown in Fig. 6. This reduction will however, be a minor influence, and Fig. 6 gives a rough approximation of the laser intensity trend involved with absorption onto the curved surface of a previous clad track.

The "ABA" melt pool shape given in Fig. 7 is the shape of the "B" track melt pools only (the "A" melt pools in the "ABA" cladding would all be similar to the initial "A" track of the "AAA" cladding discussed above). In this case, the melt front also begins later than for an "A" track, but this effect happens on both sides of the leading edge of the melt because the melt is being generated between two previously laid "A" tracks (see Figs. 1 and 2). There being two "shoulders" involved means that the relative intensity reduction discussed above happens on both sides of the melt pool, see Fig. 7.

B. Powder catchment efficiency as a function of cladding technique

Figure 5 raises points that concern the total area of the melt pool surfaces and the powder catchment efficiency for each type of cladding technique.

In the case shown in Fig. 5 for the AAA cladding, the tracks created after the first one have a similar melt pool surface area to the initial track (27.94 mm^2 compared with 27.35 mm^2 for the initial track). However, the powder catchment efficiency of the initial track is higher than for these subsequent melt pools (76% for the initial track and 67% for subsequent tracks in this case). The inferior powder catchment efficiency of the subsequent tracks is probably related to three effects;

(a) The delayed melt front on the "shoulder" side of the melt means that incoming powder would be impinging on more unmelted material and would ricochet away from the interaction zone off the solid shoulder of the previous track,
(b) The steeper, 3D sloping nature of the melt makes it less effective for powder catchment than the more straightforward 2D slope of the melt for initial track (Fig. 1), i.e., a more inclined melt surface could deflect incoming particles more effectively.
(c) The incoming gas flow and any entrained particles would be deflected only forwards off the 2D sloping melt of the initial track, where they might be reabsorbed by the moving melt. However, for subsequent tracks, the gas and any entrained particles would be deflected forwards and sideways, out of the laser-material interaction zone by the 3D slope of the melt surface.

It should be noted that the "B" track described in Fig. 6 was carried out at 1.0 m/min, whereas the "A" tracks for both "A" and AAA cladding were carried out at the lower speed of 0.7 m/min. It is, therefore, very interesting that the melt pool size was slightly larger for this track than it was for "A" or AAA tracks (29.13 mm^2), and the powder catchment efficiency was substantially increased to 99% (see Fig. 5). This is the catchment efficiency for the "B" tracks using these parameters, the overall catchment efficiency for the ABA process in this case would be the average of both the "B" track (99%) and the "A" track (76%), i.e., 87.5%. The overall catchment efficiency for AAA cladding would, however, be close to the value for tracks subsequent to the initial track, because there are usually a large number of them attached to a single initial track. The overall catchment efficiency for the AAA sample under discussion would, therefore, be only slightly over 67%.

Preheating from the deposition of the adjacent pair of "A" tracks and/or internal reflection of the edges of the laser beam toward the melt explains why the melt pool is larger for the "B" tracks. The increased powder catchment efficiency is explained in Fig. 2, as the result of improved powder capture, because the incoming powder stream rebounds off the "shoulders" of the previous tracks into the "valley" containing the melt pool.[28] Thus, the favored direction for rebounding particles in the ABA cladding is back into the melt pool, whereas in the AAA cladding, the particles which rebound tend to leave the laser-material interaction zone.

Downloaded from http://pubs.aip.org/lia/jla/article-pdf/doi/10.2351/7.0000904/16705003/012025_1_online.pdf

© Author(s) 2023

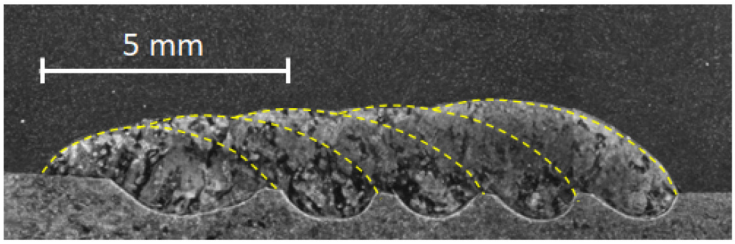

(a)

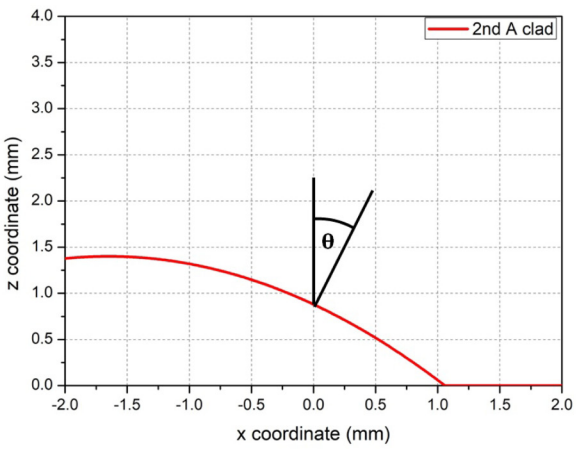

(b)

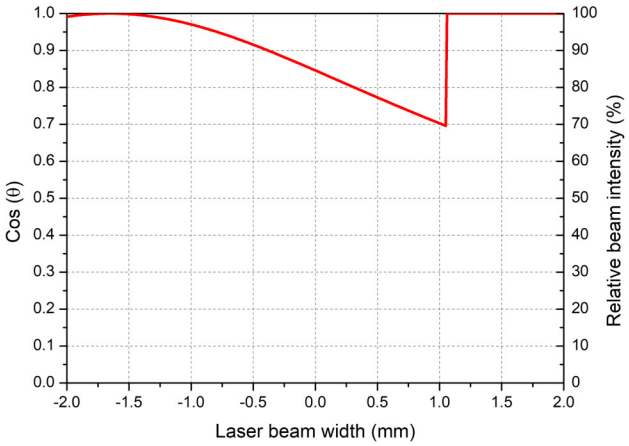

(c)

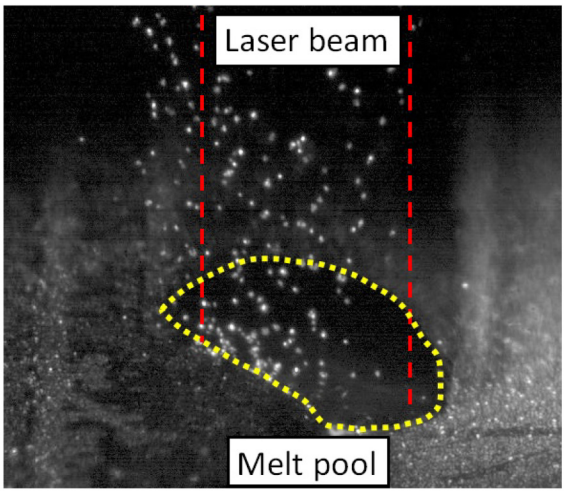

(d)

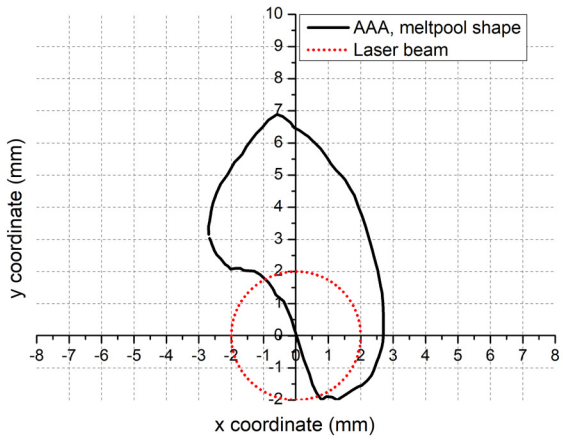

(e)

FIG. 6. Laser energy intensity is dependent on the angle of incidence on the "shoulder" of the previous track. (a) The videoed track was the third from the left in this cross section [i.e., A_3 in Fig. 1(b)]. (b) The slope of the "shoulder" of the previous track [A_2 in Fig. 1(b)]. (c) The relative beam intensity in the laser-material interaction area (proportional to the cosine of the angle of incidence, θ). (d) A frame taken from the high speed imaging video. (e) The plan view of the perimeter of the melt pool calculated from the video.

Downloaded from http://pubs.aip.org/lia/jla/article-pdf/doi/10.2351/7.0000904/16705003/012025_1_online.pdf

© Author(s) 2023

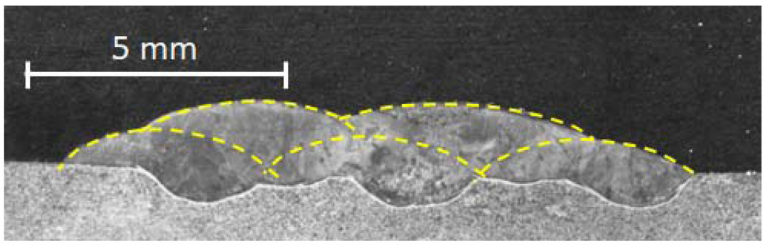

(a)

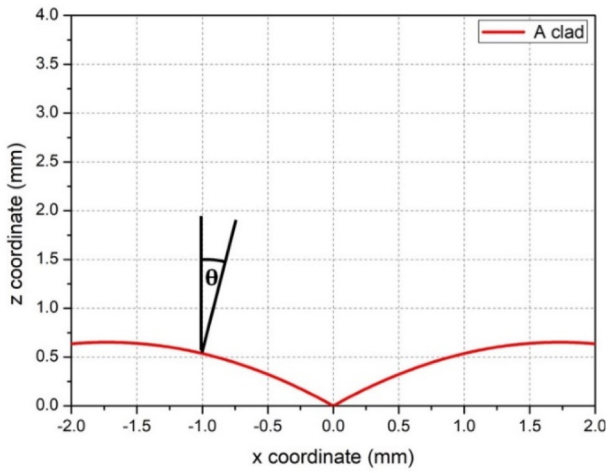

(b)

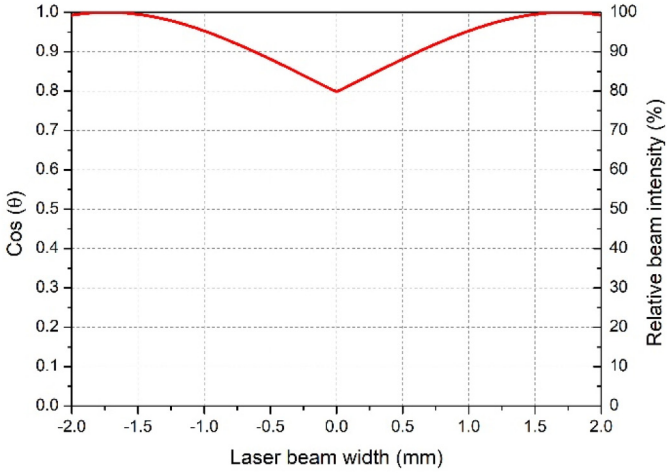

(c)

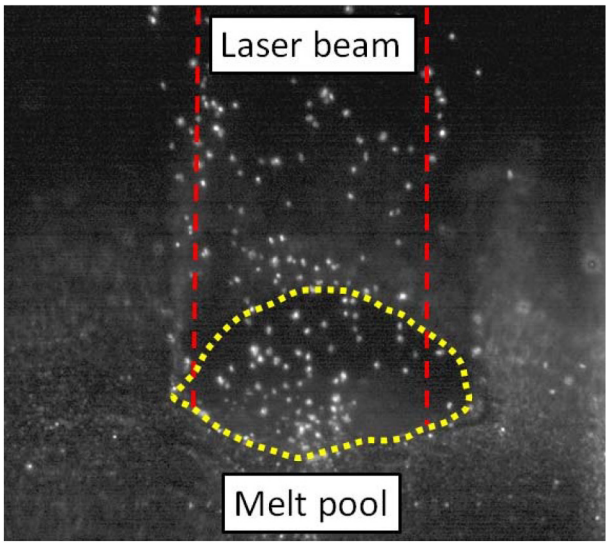

(d)

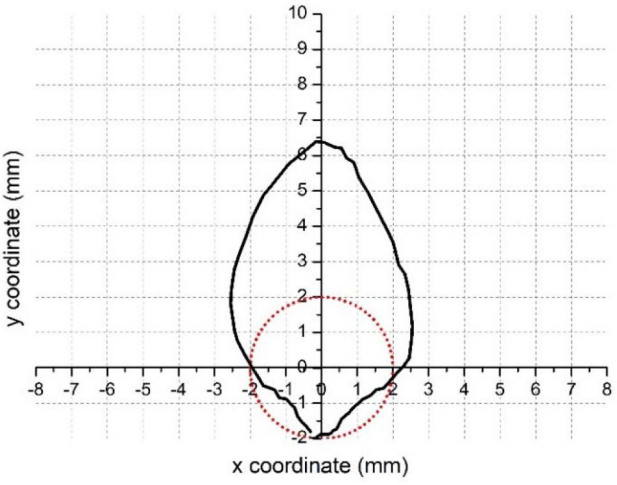

(e)

FIG. 7. Results for "B" tracks in ABA cladding. (a) The cross section of the ABA clad layer, (b) the cross-sectional geometry of the two adjacent "A" tracks, (c) The relative beam intensity reduction as a result of the "A" track curvature, (d) A single frame of the "B" track melt pool, (e) the plan view of the "B" track melt pool shape.

Downloaded from http://pubs.aip.org/jla/jla/article-pdf/doi/10.2351/7.0000904/16705003/012025_1_online.pdf

© Author(s) 2023

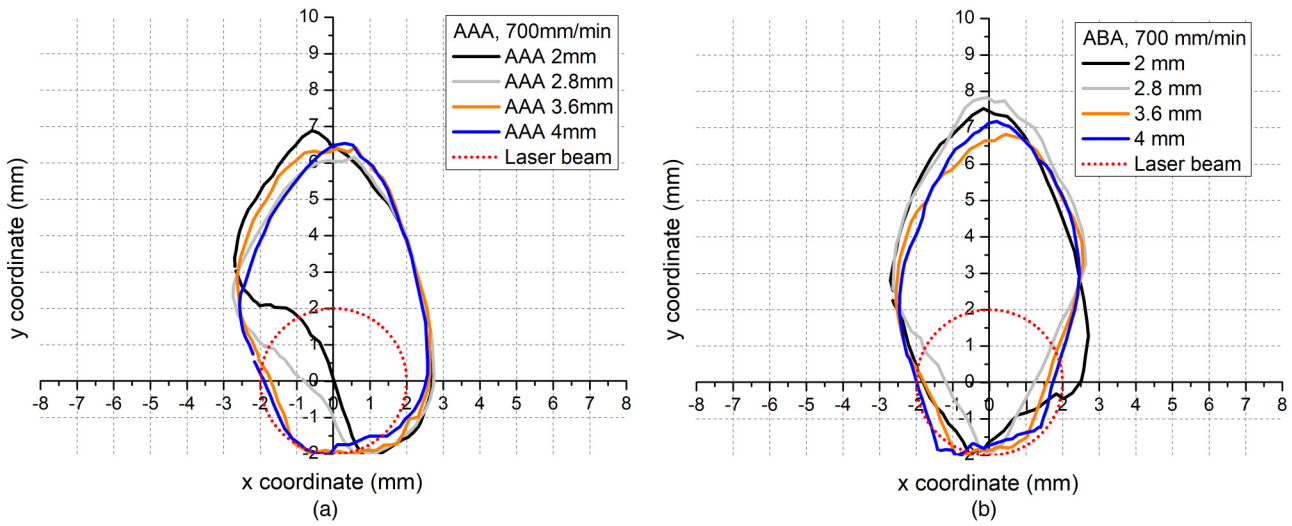

FIG. 8. Melt pool maps for AAA and ABA cladding with increasing intertrack distance.

C. Effects of changing the intertrack distance

In laser cladding, the area coverage rate of the process can be increased by increasing the process speed or by decreasing the number of tracks per unit area, which involves an increase in the intertrack distance (although other parameters may have to be increased to maintain clad layer thickness). It is, therefore, of interest to see if an increase in intertrack distance results in an improvement in powder catchment efficiency.

Figure 8 presents the melt pool maps for both AAA and ABA cladding at a process speed of 700 mm/min with center-to-center track spacings of 2, 2.8, 3.6, and 4 mm. The individual tracks were approximately 4 mm wide in cross section at the substrate surface, so a 2 mm center-to-center distance means that there was a 50% overlap of one track on the previous one. The AAA melt pool maps show that the late start of the melt front on the track overlap side of the pool (discussed above) is most pronounced when the track-to-track overlap is largest (i.e., at smaller intertrack distances). As the intertrack spacing is increased, this effect is diminished because the melt pool is exposed to more of the flat substrate surface and the melt geometry becomes more like a solo "A" track. The ABA melt pool maps present similar information for the late

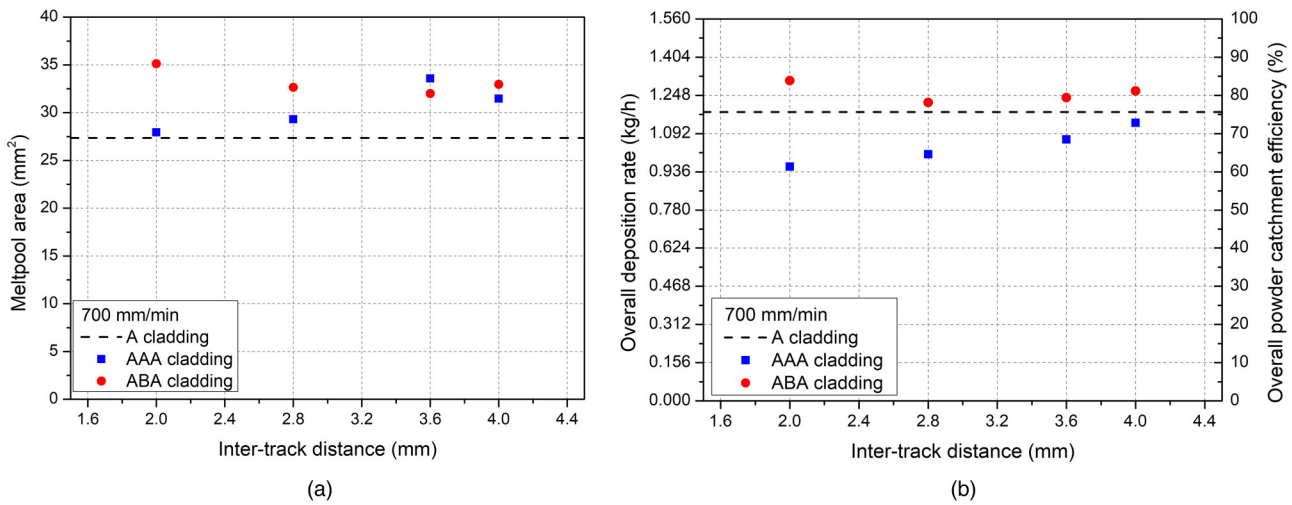

FIG. 9. Melt pool areas (from Fig. 8) and their associated powder catchment efficiencies.

Downloaded from http://pubs.aip.org/lia/jla/article-pdf/doi/10.2351/7.0000904/16705003/012025_1_online.pdf

© Author(s) 2023

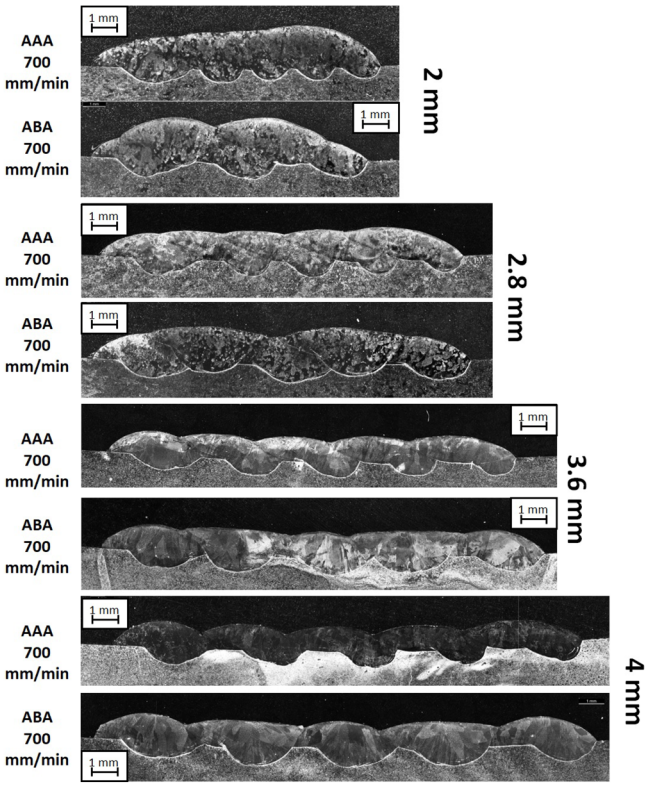

FIG. 10. Cross sections of AAA and ABA clad deposits produced with the same parameters over a range of inter-track (center to center) spacings.

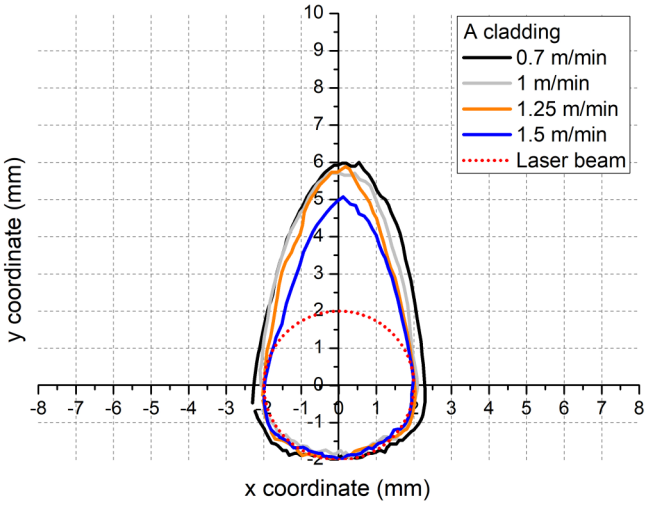

FIG. 11. Melt (plan view) for "A" tracks as a function of process speed.

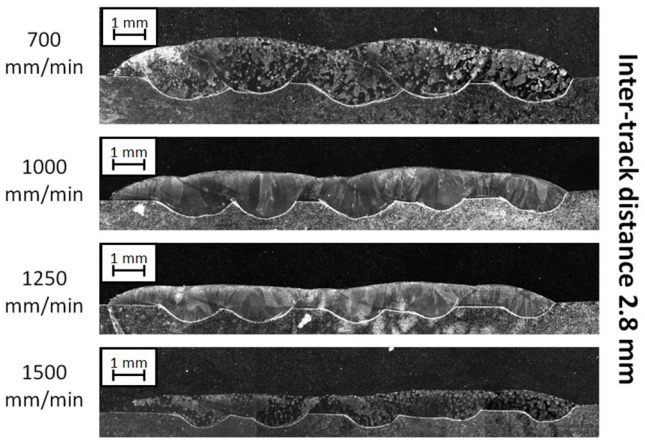

FIG. 12. Cross sections of ABA clads made at different speeds with an inter-track distance of 2.8 mm.

start of the melt (compared with solo "A" tracks) on both sides of the leading edge of the pool.

Figure 9 presents the melt pool surface areas and the powder catchment efficiency for each case shown in Fig. 8 [the result for the initial "A" track in the AAA cladding and the "A" tracks in the ABA cladding are given as a horizontal dotted line in Figs. 9(a) and 9(b)]. It is clear that, for the AAA cladding process, there is a gradual increase in melt pool area as the intertrack distance is increased, and the melt pool initiation delay caused by the slope of the previous track diminishes. For the more symmetrical ABA cladding B pools, there is no clear trend in pool size with increasing intertrack distance although the B pools are generally larger than their AAA counterparts. The B tracks of this data set also have better deposition rates than either the initial or the subsequent "A" tracks.

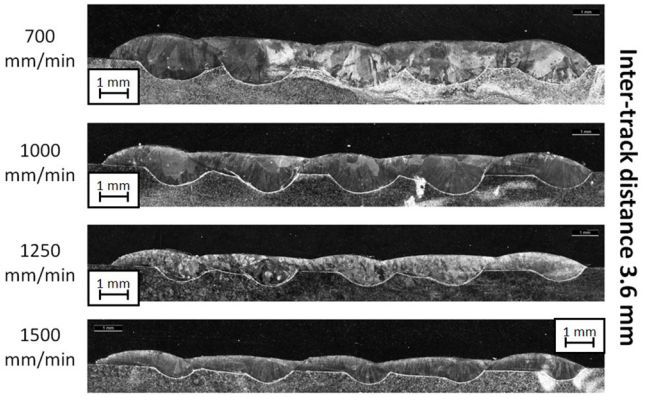

FIG. 13. Cross sections of ABA clads made at different speeds with an intertrack distance of 3.6 mm.

Downloaded from http://pubs.aip.org/lia/jla/article-pdf/doi/10.2351/7.0000904/16705003/012025_1_online.pdf

© Author(s) 2023

However, when considering the effect of inter-track distance on the process, a very important consideration is any effect on the thickness and waviness of the clad layer. This thickness and waviness determine how much useful clad layer will remain on the surface after the clad layer has been machined to a flat surface.

Figure 10 presents cross sections of the AAA and ABA samples and it is evident that, under these process parameters, both the 2 mm intertrack distance (50% track overlap) and the 4 mm distance are inappropriate choices for producing a flat clad deposit. In the 2 mm case, the clad surface is oversupplied with powder, and in the 4 mm case, the gap between tracks is insufficiently supplied.

Although both cladding techniques would result in an array of solo "A" tracks if the intertrack distance was wide enough, it is clear that an intertrack distance which is approximately equal to the melt width (4 mm) is not large enough for this to happen. The ABA process retains its superior powder catchment efficiency at this large intertrack distance because escaping powder particles are still directed back into the melt by deflection off the adjacent "A" tracks.

D. Effect of process speed on "A" tracks

For "A" clad tracks (either solo "A" tracks or the "A" tracks in ABA cladding), an increase in the cladding speed from 0.7 to 1.5 m/min had the expected result of reducing the size of the melt pool surface, as can be seen in Fig. 11.

Although the results shown in Fig. 11 represent changes over a 214% increase in the process speed, the associated (linear) reduction in melt pool surface area was only 30% (from 27 to 19 mm^2) and the (linear) reduction in powder catchment efficiency was only 9% (from 76% to 69%). At higher speeds, the laser energy produces shallower melt pools with only a limited reduction in melt pool surface area. The minor reduction in powder catchment efficiency over this large speed range clearly indicates that the melt pool surface is large enough throughout this parameter set to interact with most of the incoming powder stream. Small reductions in pool size, therefore, result in even smaller reductions in powder catchment efficiency.

E. Effect of process speed on ABA cladding

Figures 12 and 13 show cross sections of ABA clad specimens created at different process speeds, with intertrack distances of 2.8 and 3.6 mm, respectively. It is clear that the thickness of the clad layers decreases with increasing cladding speed, as would be expected.

Figure 14 gives the details of the melt pool shapes, areas, and catchment efficiencies for the examples presented in Figs. 12 and 13.

It is surprising that, over a 214% increase in cladding speed in for both intertrack distances, the shape, area, and catchment efficiencies vary only slightly. The only outlier is the size of the melt pool for the fastest speed (1.5 m/min) and largest intertrack distance (3.6 mm). Apart from this result, the melt pool areas vary by less than 10% (29.92–32.63 mm^2).

The powder catchment efficiencies for this group of results (including the melt pool size outlier) only vary by less than 5% (80%–85%). All of these ABA powder catchment efficiencies are above those of the solo "A" or multiple AAA tracks, and this demonstrates that the most important influence on powder catchment efficiency is the choice of cladding technique used, with ABA cladding giving better results than AAA.

F. Comparison of powder catchment efficiencies for AAA and ABA cladding

Many of the experimental results for ABA cladding presented so far have been dealing with "B" tracks in isolation, and an

Downloaded from http://pubs.aip.org/lia/jla/article-pdf/doi/10.2351/7.0000904/16705003/012025_1_online.pdf

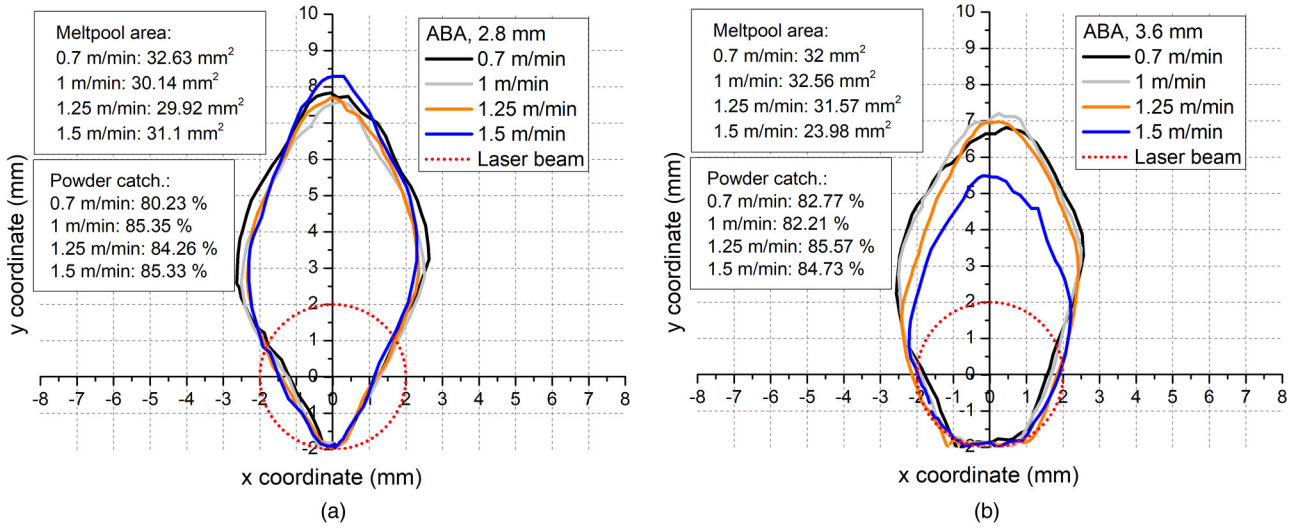

FIG. 14. Melt pool shapes, areas, and powder catchment efficiencies for the samples shown in Figs. 12 and 13.

© Author(s) 2023

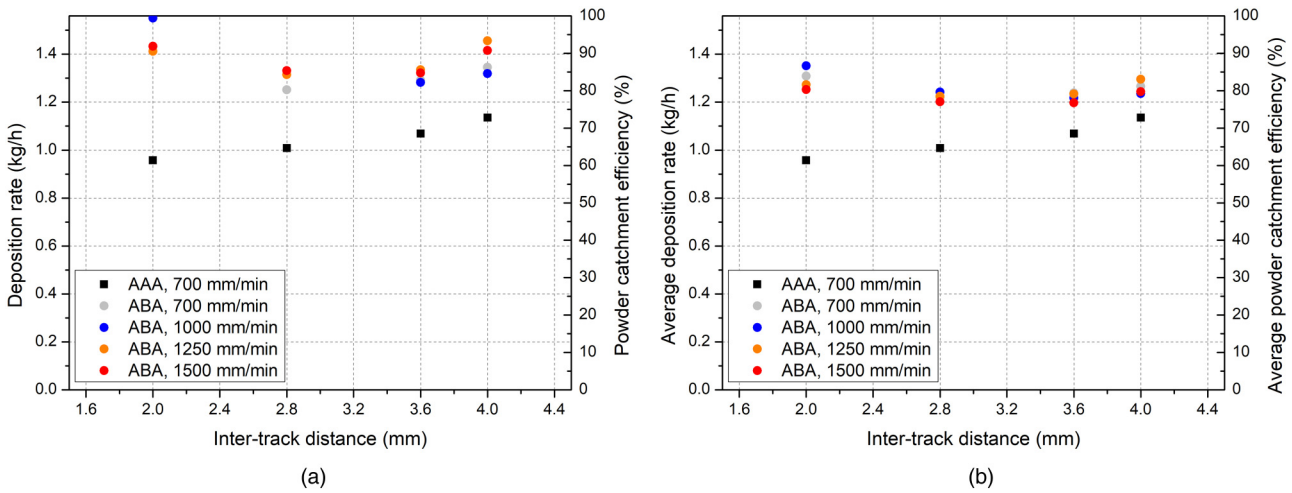

FIG. 15. Deposition rate/powder catchment efficiency results over a wide range of cladding speeds and intertrack distances for: (a) "B" tracks only, (b) ABA cladding (average of "A" and "B" tracks).

experimental data set for powder catchment efficiency for these tracks is given in Fig. 15(a).

The improvement over AAA cladding is quite clear, with one result showing a 99% powder catchment efficiency (see Fig. 5). However, this gives an exaggerated view of the powder catchment efficiency of the ABA cladding process, which is, as discussed earlier, the average of the solo "A" track efficiency for those parameters and the "B" track results shown in Fig. 15(a). These average powder catchment efficiencies for ABA cladding are presented in Fig. 15(b) and, although these values are lower than those shown in Fig. 15(a), they are still a substantial improvement over the AAA results.

IV. CONCLUSIONS

The experimental and analytical work presented here confirms the following conclusions within the parameter set used:

- Powder catchment efficiency is an important metric for laser cladding and associated DED processes.
- There is a substantial difference between the melt pool shape and the powder catchment efficiency of the initial track and subsequent tracks in AAA cladding.
- The "subsequent" tracks in AAA cladding have an asymmetrical melt pool shape as a result of the overlap of one track with the previous one. This asymmetry exposes more solid material to the incoming powder stream which decreases the powder catchment efficiency of the process.

"B" tracks in ABA cladding have an enhanced powder catchment efficiency primarily because the edges of the powder stream are reflected back into the melt pool off the "shoulders" of the adjacent "A" tracks.

- An increase in inter-track distance can improve powder catchment for AAA cladding but has no clear effect on ABA cladding powder catchment.
- Increasing cladding speed has a surprisingly small effect on weld pool size or powder catchment efficiency, although it has a substantial effect on clad layer cross section (reduced speeds result in thicker clad layers).
- ABA cladding offers a substantial improvement in powder catchment efficiency over AAA cladding and also eliminates the initiation anomalies common to AAA cladding.

AUTHOR DECLARATIONS

Conflict of Interest

The authors have no conflicts to disclose.

Author Contributions

Daniel Koti: Writing – original draft (equal); Writing – review & editing (equal). **John Powell:** Writing – original draft (equal); Writing – review & editing (equal). **Himani Naesstroem:** Writing – review & editing (equal). **K. T. Voisey:** Writing – original draft (equal); Writing – review & editing (equal).

REFERENCES

[1]J. Mazumder and J. I. Singh, "Laser surface alloying for corrosion and wear," J. High Temp. Mater. Proc. **7**, 101–106 (1986).
[2]W. M. Steen and J. Powell, "Laser surface treatment," J. Mater. Eng. **2**, 157–162 (1981).
[3]J. Powell, "Laser cladding," Ph.D. thesis (Imperial College, London University, 1983).
[4]H. Naresstroem, "Phenomena in laser based material deposition," Ph.D. thesis (Lulea University of Technology, 2021). ISBN: 978-91-7790-819-7.
[5]H. Siva Prasad, F. Brueckner, and A. F. H. Kaplan, "Powder catchment in laser metal deposition," J. Laser Appl. **31**, 022308 (2019).
[6]A. Harooni, A. M. Nasiri, A. P. Gerlich, A. Khajepour, A. Khalifa, and J. M. King, "Processing window development for laser cladding of zirconium on zirconium alloy," J. Mater. Process. Technol. **230**, 263–271 (2016).

Downloaded from http://pubs.aip.org/jla/jla/article-pdf/doi/10.2351/7.0000904/16705003/012025_1_online.pdf

© Author(s) 2023

[7]A. J. Pinkerton and L. Li, "The significance of deposition point standoff variations in multiple-layer coaxial laser cladding (coaxial cladding standoff effects)," Int. J. Mach. Tools Manuf. **44**, 573–584 (2004).
[8]S. Donadello, V. Furlan, A. G. Demir, and B. Previtali, "Interplay between powder catchment efficiency and layer height in self-stabilized laser metal deposition," Opt. Lasers Eng. **149**, 106817 (2022).
[9]C. P. Paul, P. Ganesh, S. K. Mishra, P. Bhargava, J. Negi, and A. K. Nath, "Investigating laser rapid manufacturing for Inconel-625 components," Opt. Laser Technol. **39**, 800–805 (2007).
[10]Y. S. Lee, M. Nordin, S. S. Babu, and D. F. Farson, "Influence of fluid convection on weld pool formation in laser cladding," Weld. J. **93**, 292–300 (2014); available at https://www.researchgate.net/profile/Yousub-Lee-2/publication/268278864_Influence_of_Fluid_Convection_on_Weld_Pool_Formation_in_Laser_Cladding/links/549af80b0cf2b80371371766/Influence-of-Fluid-Convection-on-Weld-Pool-Formation-in-Laser-Cladding.pdf.
[11]M. Dalaee, E. Cerrutti, I. Dey, C. Leinenbach, and K. Wegener, "Parameters development for optimum deposition rate in laser Dmd of stainless steel En x3crnimo13-4," Lasers Manuf. Mater. Process. **9**, 1–17 (2021).
[12]P. R. Bloemer, J. T. Pacheco, A. Cunha, M. T. Veiga, O. C. d. M. Filho, V. H. Meura, and M. F. Teixeira, "Laser cladding of Inconel 625 on AISI 316L: Microstructural and mechanical evaluation of parameters estimated by empirical-statistical model," J. Mater. Eng. Perform. **31**, 211–220 (2021).
[13]L. Meng, P. Sheng, and X. Zeng, "Comparative studies on the NI60 coatings deposited by conventional and induction heating assisted extreme-high-speed laser cladding technology: Formability, microstructure and hardness," J. Mater. Res. Technol. **16**, 1732–1746 (2022).
[14]V. Ocelík, M. Eekma, I. Hemmati, and J. Th. M. De Hosson, "Elimination of start/stop defects in laser cladding," Surf. Coat. Technol. **206**, 2403–2409 (2012).
[15]W. Gao, S. Zhao, F. Liu, Y. Wang, C. Zhou, and X. Lin, "Effect of defocus manner on laser cladding of Fe-based alloy powder," Surf. Coat. Technol. **248**, 54–62 (2014).
[16]S. Liu, P. Farahmand, and R. Kovacevic, "Optical monitoring of high power direct diode laser cladding," Opt. Laser Technol. **64**, 363–376 (2014).
[17]J. C. Heigel, M. F. Gouge, P. Michaleris, and T. A. Palmer, "Selection of powder or wire feedstock material for the laser cladding of Inconel® 625," J. Mater. Process. Technol. **231**, 357–365 (2016).
[18]J. Tuominen, Jonne Näkki, Henri Pajukoski, Tuomo Peltola, and P. Vuoristo, "Recent developments in high power laser cladding techniques," Int. Congr. Appl. Lasers Electro-Opt. **2012**, 192–196 (2012).
[19]Y. Liu, L. Yang, X. Yang, T. Zhang, and R. Sun, "Optimization of microstructure and properties of composite coatings by laser cladding on titanium alloy," Ceram. Int. **47**, 2230–2243 (2021).
[20]M. Pellizzari, Z. Zhao, P. Bosetti, and M. Perini, "Optimizing direct laser metal deposition of H13 cladding on cube alloy substrate," Surf. Coat. Technol. **432**, 128084–128100 (2022).
[21]G. A. Turichin, E. V. Zemlyakov, E. Y. Pozdeeva, J. Tuominen, and P. Vuoristo, "Technological possibilities of laser cladding with the help of powerful fiber lasers," Met. Sci. Heat Treat. **54**, 139–144 (2012).
[22]E. Govekar, A. Jeromen, A. Kuznetsov, G. Levy, and M. Fujishima, "Study of an annular laser beam based axially-Fed powder cladding process," CIRP Ann. **67**, 241–244 (2018).
[23]S. Sun, Y. Durandet, and M. Brandt, "Parametric investigation of pulsed Nd: YAG laser cladding of stellite 6 on stainless steel," Surf. Coat. Technol. **194**, 225–231 (2005).
[24]J.-D. Kim, E.-J. Lee, and J.-G. Whang, "Comparison of clad layer characteristics with overlapping criterion in multi pass laser cladding," J. Korean Soc. Mar. Eng. **40**, 768–773 (2016).
[25]T. Ge, L. Chen, P. Gu, X. Ren, and X. Chen, "Microstructure and corrosion resistance of Tic/Inconel 625 composite coatings by extreme high speed laser cladding," Opt. Laser Technol. **150**, 107919–107931 (2022).
[26]J. D. Kim, E. J. Lee, and C. G. Kim, "Study on laser cladding of heat resisting steel using EuTroLoy 16006 powder (II)-characteristics of alloying elements distribution of multi pass clad layer," Trans. Korean Soc. Mech. Eng. A **41**, 307–312 (2017).
[27]D. Salehi and M. Brandt, "Melt pool temperature control using Labview in Nd:YAG laser blown powder cladding process," Int. J. Adv. Manuf. Technol. **29**, 273–278 (2005).
[28]C. Zhong, N. Pirch, A. Gasser, R. Poprawe, and J. Schleifenbaum, "The influence of the powder stream on high-deposition-rate laser metal deposition with Inconel 718," Metals **7**, 443–456 (2017).
[29]D. Koti, J. Powell, and K. T. Voisey, "Improving laser cladding productivity with 'ABA' cladding," Proc. CIRP **111**, 205–209 (2022).

Downloaded from http://pubs.aip.org/jla/jla/article-pdf/doi/10.2351/7.0000904/16705003/012025_1_online.pdf

© Author(s) 2023